

REDUCTION OF EMISSIONS FROM A HIGH SPEED FERRY

Gregory J. Thompson, Mridul Gautam, Nigel N. Clark, Donald W. Lyons,
Dan Carder, Wesley Riddle, Ryan Barnett, Byron Rapp and Sam George
National Center for Alternative Fuels, Engines and Emissions
West Virginia University

ABSTRACT

Emissions from marine vessels are being scrutinized as a major contributor to the total particulate matter (TPM), oxides of sulfur (SO_x) and oxides of nitrogen (NO_x) environmental loading. Fuel sulfur control is the key to SO_x reduction. Significant reductions in the emissions from on-road vehicles have been achieved in the last decade and the emissions from these vehicles will be reduced by another order of magnitude in the next five years: these improvements have served to emphasize the need to reduce emissions from other mobile sources, including off road equipment, locomotives, and marine vessels. Diesel-powered vessels of interest include ocean going vessels with low- and medium-speed engines, as well as ferries with high speed engines, as discussed below.

A recent study examined the use of intake water injection (WIS) and ultra low sulfur diesel (ULSD) to reduce the emissions from a high-speed passenger ferry in southern California. One of the four Detroit Diesel 12V92 two-stroke high speed engines that power the Waverider (operated by SCX, inc.) was instrumented to collect intake airflow, fuel flow, shaft torque, and shaft speed. Engine speed and shaft torque were uniquely linked for given vessel draft and prevailing wind and sea conditions. A raw exhaust gas sampling system was utilized to measure the concentration of NO_x, carbon dioxide (CO₂), and oxygen (O₂) and a mini dilution tunnel sampling a slipstream from the raw exhaust was used to collect TPM on 70 mm filters. The emissions data were processed to yield brake-specific mass results. The system that was employed allowed for redundant data to be collected for quality assurance and quality control. To acquire the data, the Waverider was operated at five different steady state speeds. Three modes were in the open sea off Oceanside, CA, and idle and harbor modes were also used.

Data have showed that the use of ULSD along with water injection (WIS) could significantly reduce the emissions of NO_x and PM while not affecting fuel consumption or engine performance compared to the baseline marine diesel. The results showed that a nominal 40% reduction in TPM was realized when switching from the marine diesel to the ULSD. A small reduction in NO_x was also shown between the marine fuel and the ULSD. The implementation of the WIS showed that NO_x was reduced significantly by between 11% and 17%, depending upon the operating condition. With the WIS, the

TPM was reduced by a few percentage points, which was close to the confidence in measurement.

INTRODUCTION

Emissions from off-road equipment are being examined in more detail and have been the focus of research over the last five years. For example, many studies and retrofit programs have been completed for construction equipment. Recently, locomotive emissions have come under regulations. Emissions from marine vessels are the next area of interest to reduce atmospheric loading from the transportation sector. Specifically, reduction of marine emissions offer an avenue for improving air quality in coastal cities and along inland waterways



Fig. 1 The SCX, Inc. WaveRider ferry.

In-use brake-specific mass exhaust emissions rates were determined for a high-speed hydrofoil ferryboat, the WaveRider. This vessel operates between Oceanside and San Diego, CA as a passenger ferrying service for commuters living north of San Diego. The ferry operates a single round-trip service during the weekday, departing from Oceanside in the morning to arrive in San Diego for the morning commute, and then leaving San Diego in the evening for a return trip to Oceanside. The vessel employs a retractable hydrofoil to achieve high speeds. A picture of the WaveRider is shown in Fig. 1 with the hydrofoil deployed. The ferry was approximately 80 feet in length and was powered by four high-

speed Detroit Diesel 12V92 two stroke compression ignition engines.

One pair of the engines was located on the port side and the other pair was located on the starboard side. Each pair of engines was connected to a gearbox. The output shaft from each gearbox was used to drive a water jet propulsion system. For each set of engines, one was located fore and the other was located aft in a staggered arrangement. Figure 2 presents a photograph of the starboard engine pair. The engines incorporate two turbochargers, located on either side of the engine. The outlet of the turbocharger feeds two superchargers. A water injection system (intake fumigation) was incorporated between the turbocharger outlet and supercharger inlet. The water injection control was such that the system was deactivated if the manifold air pressure was below a certain value. Therefore, no water injection data was available for the idle and harbor set points. Water was also injected in the exhaust to reduce exhaust system temperatures. The water was injected downstream of the turbocharger outlet, after an elbow (above the forward engine out shaft) as shown in Fig. 2.



Fig. 2 Photograph of both starboard engines. The forward engine is on the left side of the picture and the aft engine is on the right side. The output shaft of the forward engine is shown in the foreground.

The vessel and engines were designed to use conventional marine compression ignition fuel (off-road diesel). Typical marine fuel for high-speed diesel engines is similar to other off-road fuel except that sulfur concentration levels may be as high as 5000 ppm. The fuel was stored in two 800-gallon tanks. There was some uncertainty regarding the exact construction of the fuel storage tanks, but it appears as though the two tanks were constructed from aluminum plates welded together with a center divider plate.

In an effort to reduce the oxides of nitrogen (NO_x) emissions generated from these engines, a water fumigation system was installed in the intake to add additional humidification. To reduce particulate matter (PM), low sulfur diesel fuel was used in place of the higher sulfur-level marine diesel. The water injection system was supplied and installed by M.A. Turbo/Engine, Ltd. [1]. The low sulfur diesel (LSD) fuel was supplied by BP and is designated as BP ECD[®]. The testing consisted of examining the emissions produced by the starboard, forward engine when it was fueled with marine fuel and with LSD fuel. In addition, for each fuel, the emissions were measured with and without the water injection system activated, thus making a total of four different engine

configurations. For each of these four configurations, the engine was operated at four different speeds to evaluate the emissions, namely, idle (650 rpm), 1900 rpm, 2000 rpm, and 2100 rpm.

The purpose of this study was to measure engine emissions reduction of oxides of nitrogen (NO_x), which resulted from implementation of an intake water injection system, and total particulate matter (TPM), which was afforded by changing from marine diesel (high sulfur) to a lower sulfur fuel. The emissions reduction program was in support of the “Project 81, Governor’s Congestion Relief Program – High Speed Low-emissions Ferry Demonstration” granted to the Unified Port District of San Diego. Fuel consumption (FC) was also measured to determine if there was a fuel penalty associated with either the fuel change or implementation of the water injection system. For this testing, West Virginia University designed and developed a raw emissions sampling system, according to recommendations provided by Title 40 CFR 86, Title 40 CFR 89, Title 40 CFR 92, Title 40 CFR 94, ISO8178, and SAE J177 [2-7], where applicable. Although some recent efforts have advocated a standard marine emissions protocol 2003 Marine Environment Engineering Technology Symposium because precise methods are not yet specified and that transient in-use emissions still pose logistical problems [8, 9]. The test engine specification is listed in Table 1. All emissions tests were performed on the Pacific Ocean outside the marina at Oceanside, CA.

Table 1 Forward starboard engine specifications.

Engine Manufacturer	Detroit Diesel Corp.
Engine Model	12V92
Model Year	1981
Displacement (cu. in.)	1104
Power Rating (hp)	1080 hp @ 2300 rpm
Configuration	12V92
Bore (in.) x Stroke (in.)	4.84 x 5.00
Induction	Turbocharger with Blower
Fuel Type	Diesel
Engine Strokes per Cycle	Two
Injection	Mechanical

Representatives from SCX, Inc. provided and operated the ferryboats and supervised fueling, while West Virginia University (WVU) provided and operated the emissions measurement equipment. Measurements were done while the ferry was not in normal service. The computed results of the emissions tests are summarized in this paper.

OVERVIEW OF MEASUREMENT SYSTEM

The following section is included in order to outline the equipment and procedures used for the evaluation of the ferryboat engine exhaust emissions. Due to space limitations and the nature of in-use emissions testing, particular attention was paid to the selection of the analytical equipment. WVU designed and developed a raw exhaust emissions sampling and measurement system that would provide the highest possible accuracy. In particular, analyzers and transducers were selected that would provide levels of accuracy specified in the

above documents without being adversely affected by the vibrations encountered during normal operation of the ferry.

Particulate Sampling System

The primary goal of engine emissions testing was to determine the effects that exhaust constituents have on the environment. In order to simulate “real world” conditions and to produce accurate particulate matter measurements, it was necessary to mimic the dilution process that occurs when hot exhaust gases mix with ambient air. However, it should be noted that for this ferry the raw exhaust was flooded with water to cool the exhaust and was ported to the side of the vessel at the water line. Therefore, the exhaust from the engines from this vessel never does mix with ambient air, as was the case for most land-based and many marine engines. However, measurement of PM is traditionally accomplished with dilution of the raw exhaust. The effects of exhaust gas dilution with the ambient are threefold, with the primary reason being provision for exhaust-air interactions that would normally take place at the exhaust outlet. In addition, the dilution process quenches post-cylinder combustion reactions and lowers the exhaust gas dew point, thus inhibiting condensation.

The dilution tunnel used for this research was of a partial-flow design, where a measured amount of exhaust gas emitted by the test engine was routed into the tunnel and mixed with a regulated amount of HEPA-filtered, conditioned dilution air in order to achieve desired dilution ratios. The raw exhaust sample probe is described below. The system was mass-flow controller based, but uses conditioned, time-aligned raw and dilute CO₂ tunnel concentrations to infer dilution ratios and exhaust sample inlet flow rates. The dilution tunnel, which was approximately 2 inches in diameter and 24 inches in length, was constructed of stainless steel to prevent oxidation contamination and degradation. The dilution air supply was provided by a rotary-vane pump, and was HEPA-filtered and cooled to remove water and maintain near-ambient temperatures. The exhaust gases entered the tunnel at its centerline and passed through a mixing orifice plate that was close-coupled to the divergent tunnel entrance. The orifice plate creates turbulence in the flow path that promotes thorough mixing. In addition, tunnel flow rates were maintained sufficiently high so as to promote fully-developed, blunt-shaped turbulent flow profiles that reduce the sensitivity of point-source sample probe placement. The full tunnel flow stream was pulled through a stainless steel filter holder that contains two Pallflex 70mm diameter Model T60A20 fluorocarbon-coated glass microfiber filters in series. Two filters, a primary and a secondary, were used in the filter holder to maximize filter trapping efficiency. The diluted sample stream was maintained at temperatures below 125°F, measured at the inlet of the PM filter holder. The purpose of this was to keep the face of the particulate sample filter at a sufficiently low temperature so as to prevent any physical damage to the filter material or stripping of volatile components that would normally condense upon the filter surface.

Sierra mass flow controllers provided flow rate control of the total flow and dilution air based on computer voltage outputs. The mass flow controllers were recalibrated by the manufacturer and additionally checked with Merriam Instruments laminar flow elements. The deduction of dilution ratio was provided through the measurement of dilute and raw

CO₂ concentrations in the dilution tunnel. Exhaust sample flow rates into the tunnel were inferred from dilution ratio measurements and total mass flow rates measured with the mass flow controllers. This provided redundant measurements that helped to insure accurate dilution ratio measurements.

The PM from the diluted exhaust stream of the tunnel was used to infer the mass of PM emitted by the engine during a given test cycle. PM collected on the filter consists primarily of elemental carbon as well as sulfates, the soluble organic fractions (SOF), engine wear metals and bound water. The sample filters were conditioned in an environmentally controlled chamber to 70°F and 50% relative humidity, in compliance with requirements of CFR Parts 86 and 89 [2, 3], and weighed before and after sample collection using a Cahn C-32 microbalance. However, for this research effort, the filters were pre-weighed at the Engine and Emissions Research Laboratory (EERL) at WVU and shipped to the test site in individually labeled petri dishes. After the filters were used, they were shipped back to the EERL and reconditioned and the final weight recorded. The required times set forth in CFR Parts 86 and 89 [2, 3] were not followed. However, previous experience with gravimetric PM analyses performed at remote sites indicates minimal, if any, variations due to non-standard PM conditioning constraints as long as the filters were conditioned for the prescribed amount of time.

Gaseous Emission Sampling System

The sampling system originated with stainless-steel sample probes that were mounted in the raw exhaust stack just after the turbocharger. These multi-hole, stainless-steel probes were designed according to the recommendations included in CFR 40 Part 89, Subpart E [3]. Due to the direct injection of water to cool the exhaust and dual turbochargers, exhaust samples were pulled from each engine exhaust bank and merged together to obtain an average engine exhaust composition. Due to the divorced twin turbocharger arrangement, intake manifold pressures were observed to insure that equal amounts of exhaust flow were being supplied from each engine bank so as to prevent measurement bias when using this integrated sampling procedure. Heated sample lines were used from the probe to the measurement system located on the main deck. The wall temperatures of the filter assembly and the heated sample transport lines were electrically heated and maintained at a temperature of 375±10°F using electronic temperature controllers. This temperature set point, prescribed by CFR 40, Parts 86 and 89 [2, 3], prevents the high molecular weight hydrocarbons from condensing in the sample line. It is noted that THC's were not measured for this project due to the concerns of needing compressed hydrogen on board for a flame ionization detector. It is also noted that diesel engines typically have very low HC emissions relative to the other carbon compounds (CO and CO₂) and that only NO_x and PM were the targeted compounds. The heated sample lines transported the exhaust sample to the emissions sample conditioning system. The heated line was joined with a tee with one leg going to the gaseous sampling system and the other leg going to the particulate matter mini dilution tunnel.

The gaseous sampling system incorporated a heated filter assembly, a heated-head pump, an external NO₂ converter, flow control devices, and a sample moisture control system. The flow rate controllers were implemented to provide a constant,

pulsation-damped sample for the gas analyzers, since sample pressure fluctuations can compromise measurement accuracy. Sample humidity control was used to prevent the interference effects of water – a common problem for non-dispersive infrared (NDIR) gas analyzers.

The gas analysis bench housed both NO_x and CO₂ analyzers. A brief description of each analyzer and its components, as well as theory of operation is included in this section. The entire sampling system used was compared against a full-scale dilution tunnel and engine dynamometer that conforms to CFR 40 Part 86, Subpart N and Part 89, Subpart D [2, 3]. The basis of the gaseous emissions sampling system is described in more detail elsewhere but is summarized here [10-13].

Oxides of Nitrogen Analyzer

Electrocatalytic analyzers measure oxygen concentrations based on a flow of electrons across a solid zirconium oxide (ZrO₂) catalytic electrolyte. ZrO₂ allows the transfer of O₂ ions when heated to approximately 700°C. A current is generated if the electrolyte is placed between gases of two different concentrations. Oxygen sensors of this type are the standard in the automotive industry for feedback control of air-fuel ratio. This principle may also be used to measure concentrations of other gases. NO is measured by first removing O₂ from the sample and then causing the NO to dissociate into N₂ and O₂. Oxygen is removed from the sample through a ZrO₂ electrolyte coated with platinum to catalyze the transfer process. Current must be supplied in this case because the oxygen is being transferred in the opposite direction of the flow that would be induced by the concentration gradient. The sample then flows into a second cavity where the O₂ produced from the dissociation process is measured with a second electrocatalytic device of the same design as the first. Zirconium oxide sensors typically have a T₉₀ response time of less than one second for NO. Although zirconium oxide sensors do respond to some NO₂ it is advisable to still use an NO₂ to NO converter to obtain total NO_x measurement. The sample can be filtered to prolong the sensor's life. A Horiba MEXA120 was used for this work.

Electrochemical (EC) or polarographic analyzers are a relatively simple and inexpensive method of measuring concentrations of emission gases including NO, NO₂, NO_x, SO₂, CO, O₂, and CO₂. An electrochemical cell consists of two or more electrodes separated by an electrolyte. For a cell with two electrodes, one electrode must be porous so the gas can pass through it after diffusing through a membrane. A resistor is connected between the two electrodes and voltage drop across the resistor is converted to gas concentration. If the rate of diffusion is controlled via a membrane, the current flowing through the resistor and therefore, the voltage drop across the resistor is proportional to the concentration of candidate gas, as stated by Fick's law of diffusion. Electrochemical cells typically have a T₉₀ response time of at least 5 seconds for NO. An NO₂ to NO converter is required to obtain total NO_x measurement. The sample must be filtered to avoid clogging of the membrane.

The MEXA 120 and EC cells are inherently linear by nature, but the linearized response was validated through calibration curves that were generated before each testing session began. These calibration curves were generated by using a capillary-flow gas divider and component gases mixtures that were traceable to the standards set forth by the

National Institute of Standards and Technology (NIST). The EC cell was used as a quality assurance quality control check and the results presented in this paper are only for the ZrO₂ sensor.

Carbon Dioxide Analyzer

Gaseous constituents of CO₂ were measured with a Horiba BE-140 non-dispersive infrared (NDIR) gas analyzer. NDIR analyzers operate using the principle of selective infrared light absorption – where a particular gas will absorb a certain wavelength of light within the infrared spectrum, while the other spectral wavelengths are able to transmit through the gas. The analyzer detects the amount of infrared energy able to pass through the sample gas and uses it in the determination of the concentration of the measured absorbent gas in the sample stream. An NDIR analyzer is inherently non-linear by nature, so linearized calibration curves were generated for the analyzers before each testing session began. These calibration curves were generated by using a capillary-flow gas divider and component gases mixtures that were traceable to the standards set forth by the NIST.

Fuel Flow Rate

Continuous direct fuel flow measurements were made using two Micro Motion CMF025 flowmeters with RFT9739D4SUA transmitters. One unit provided information regarding the supply side, while the other unit collected fuel flow rate data for the return side. The calibration constants supplied by the manufacturer for each sensor were entered into the WVU data acquisition (DAQ) program.

Intake and Exhaust Flow Rates

Two different means were used to measure or infer the intake and exhaust flow rates through the engine. The first method employed a Meriam laminar flow element place in the intake stream of the engine. The absolute pressure, differential pressure, and exhaust temperatures were recorded and stored with the WVU DAQ. These transducers were calibrated at WVU prior to the testing and the calibration checked at the test site. The second method was inference of exhaust flow rates through direct fuel flow measurements and carbon balance (in this case only CO₂), using exhaust CO₂ measurements. The second method was used as a quality assurance quality control check and the results presented in this paper are only for the laminar flow element.

Shaft Speed/Torque

Engine shaft speed and torque was measured using an Advanced Telemetrics International Model 2025B-S transmitter and receiver. A radio frequency (RF) signal was transmitted from the shaft in the engine compartment area to the receiver located on the lower deck seating area of the ferry. The signals from the receiver were connected into the WVU DAQ. The load cell for the torque was installed on the existing driveshaft and calibrated on-board using a shaft locking system and dead weights. The calibration of shaft speed was confirmed with the engine speed display.

The method of calibrating the shaft load cell is illustrated in Fig. 3. The load cell was installed onto the shaft and is visible on the right-hand side of the left picture. The shaft was locked in place by a fabricated arm that was bolted to the drive flange at the shaft and contacted the hull of the vessel. At the other end of the shaft, before the connection with the

transmission, a second fabricated arm was bolted to that drive flange. Pre-weighed masses were then placed on this calibration arm to calibrate the load cell. The response of the load cell was recorded for the known weight.

The shaft speed sensor was damaged beyond repair during the first day of testing. The cause of the damage was determined to be impact of the magnetic pickup against the RF collar on the rotating driveshaft. The magnetic sensor was rigidly attached to the engine frame and the mating sensor was placed on the drive shaft in the RF housing. It was determined that the fiberglass haul of the ferry distorted during high speed operation, resulting in a relative movement of the pickup and RF housing, causing the two to come into contact and breaking. Therefore, the engine tachometer on the dash of the bridge was used to determine engine speed, which as logged manually.



Fig. 3 Load cell calibration arm and lock. The top photograph illustrates the shaft locking mechanism as shown in the middle of the picture. The bottom photograph illustrates the load arm extending from the shaft and over the generator. Pre-weighed masses were used to obtain different load points for the calibration.

Additional Data

Additional data included the ambient pressure, temperature, and humidity. Vessel speed was also recorded from a Garmin GPS 35/36 unit to obtain speed over the water. It is recognized that GPS data does not provide sufficient information to relate engine load to vessel speed due to wind loading, water current, or sea state. However, it does give some qualitative information about the test. These signals were recorded and stored into the WVU DAQ. Additionally, manual

data were recorded from the vessel and included vessel GPS speed and the forward and aft starboard engine parameters of engine speed, oil pressure, water temperature, and intake (between turbocharger and supercharger) pressure on both banks. Additionally, the test engine’s post turbocharger exhaust temperatures were recorded.

Instrumentation Control/Data Acquisition

Data acquisition was controlled with software developed by WVU. National Instruments E-series data acquisition boards with a minimum 12-bit resolution were used along with an SC-2345 signal conditioning unit. All analog data were recorded in raw voltage form at a minimum of 10 Hz and later converted to engineering units with a reduction program developed in-house at WVU. In addition, GPS data was recorded and stored to disk at 1 Hz.

FERRYBOAT TEST CYCLE

Steady-state engine operating points were utilized for the emissions testing. The engine speed was reported from the panel mounted in the dash on the second deck. All testing was performed on the Pacific Ocean just offshore of Oceanside, CA. For the tests, nominal engine speeds of 1900, 2000, 2100 rpm and idle were selected as representative operating points. These points were selected since the ferry typically operates at 2100 rpm under calm conditions and between 1900 to 2100 rpm under rougher sea conditions. Sufficient vessel speed, associated with engine operation above 1900 rpm, was necessary for adequate hydrofoil operation. Idle conditions were also targeted since the engines idle during warm up, prior to leaving the dock, and after docking. To reiterate, testing was performed with baseline marine fuel and LSD fuel, as well as operation on each fuel with and without water injection. Table 2 details the test matrix. As shown in this table, a low speed marina operating mode was included for the marine fuel. This point was a no-wake speed (idle with the transmission engaged) as the ferry entered or exited the marina.

Table 2 Test configuration set points.

Fuel	Engine Speed (rpm)	Water Injection
LSD	650 (Idle)	Off
	1900	Off **
	2000	On / Off
	2100	On / Off
Marine	650 (Idle)	Off
	650 (Marina)	Off
	1900	On / Off
	2000	On / Off
	2100	On / Off

** Torque sensor failure during the WIS modes.

It is noted that the 1900 rpm set point for the LSD fuel had a failure in the load cell for the torque measurement. Because of time constraints, this point was not repeated after the load cell was fixed. The reason for the failure was a broken solder connection between the strain gauge and the RF transmitter broke.

Repeats were performed at each engine set point. Due to the nature of in-use marine testing, it was impossible to control the load on the engine (or engines) at a fixed engine speed; the load applied to the engine was a function of the requirements

set forth by the ferry operation (passenger loading, wind, current direction, speed, etc.). Therefore, the loading on the engine(s) could vary from set point-to-set point since no effort was made to reproduce the exact path of the ferry for each set point. However, engine speed was the primary variable in determining load. The data collection procedure consisted of operating the ferry at a constant engine speed for a short duration (approximately five minutes). After the emissions had stabilized, data collection commenced. The duration of the data collection was dependant upon the PM filter loading. The test times were varied according to the expected filter loading and from examining the pressure drop across the filter.

DATA REDUCTION METHODOLOGY

The research performed for this study involved in-use emissions evaluation from an engine in a marine vessel. Although there were no specific standards that outline procedures for testing of this nature, data reduction procedures outlined in Title 40 CFR 86, Title 40 CFR 89, Title 40 CFR 92, Title 40 CFR 94, ISO8178, and SAE J177 were followed, where applicable, in the experimental setup and data evaluation [2-7]. The computation of the mass emissions emitted from the engine in the ferry can be determined from the sources listed above. Generally, knowledge of the intake air flow rate and fuel flow rate (or exhaust flow rate) and the concentration level of the exhaust constituents are required. The method of reporting the mass flow through the engine used for this work was direct intake flow with a laminar flow element meter.

Mass rates of each exhaust constituent were determined from associated measured concentration levels in the exhaust and measured fuel mass flow rates, as defined in Title 40 CFR 92 [4]. The data from the last 60 seconds of each steady-state point were averaged and used for the gaseous emission analysis. For PM, the entire duration of the sampling period was used for the determination of the TPM.

The mass emission rate of NO_x was corrected for ambient temperature and humidity according to procedure outlined in Title 40 CFR 89 [3]. The particulate matter mass rate was determined from knowledge of the partial flow dilution tunnel dilution ratio, particulate filter net mass, integrated flow across the filter during the test, and the average exhaust flow rate. The particulate matter mass rate is analogous to that given in ISO8178 [6].

The flow across the filter was determined from integrating the measured flow through the mass flow controller on the mini dilution tunnel. The net filter mass was the sum of the PM loading on the primary and secondary filter. The average exhaust flow rate was determined from the measured in-field method.

RESULTS

Care must be exercised when reviewing the data for the LSD fuel (BP ECD[®]). The fuel analysis for the LSD fuel shows far higher (320 ppm) sulfur concentration than that associated with the advertised fuel properties as shown in Table 6. However, it was still an order of magnitude lower than of the marine fuel. It was possible that during the fuel extraction from the tank that the sample was contaminated due to the piping configuration connecting the two tanks and the location of the sample valve. However, the sampling line was purged

before the sample was collected and was not believed to be the source of contamination. The ferry had what appeared to be two separate tanks. It was confirmed through subsequent testing by the operator that the two tanks were indeed fully separated and that sloshing should not have occurred from the tank with the marine fuel to the tank containing the low sulfur diesel. Another possible source of contamination could have been from the process of purging the tank used for the low sulfur fuel. Prior to emissions testing, a plan was developed to fill both tanks with LSD fuel and refill enough times to approach the BP ECD[®] sulfur level. Approximately a week before the emissions testing, the port tank was filled with marine fuel. The starboard engines were then fueled with the low sulfur fuel and the port engines were fueled with the marine fuel. The ferry was then operated over its normal service and the two tanks filled with their respective fuels. Hence, at each refilling, the contamination level in each tank would diminish. The final source of contamination could have occurred during the fuel sulfur analysis.

Table 3 displays the manual data collected from the forward and aft starboard engines. As illustrated in this table, the forward and aft engines appear to have been operating at a similar load as indicated by the engine speed, oil pressure, water temperature, and turbocharger pressure. It is noted that the one exhaust temperature (T₂) on the test engine malfunctioned and was not recorded – these tabular entries are highlighted. Other data points not recorded are also highlighted. It was observed that the exhaust temperatures were typically lower when the water injection system was active than when the water injection system was disabled. This was attributed to the fact that lower in-cylinder temperatures were obtained with the water injection. This was also supported by the lower NO_x emissions discussed below. The exhaust temperature data for the harbor runs may appear to be confusing. As shown for M010126-1 and M010130-1 the temperatures continued to drop throughout the testing. This was due to the fact that the ferry was entering the marina from the ocean at full power and the engine was at normal operating temperature. The engine coolant and oil began to cool during these tests. However, the temperature for the other harbor run, M010127-1, was for the ferry leaving the dock, thus the engine was at its normal idle operating temperature and did not change during the test since there was minimal load on the engine.

Tables 4 and 5 illustrate the average data from test for the vessel underway and at the dock, respectively. The average data from these tables are plotted in Figs. 4 to 7. The “error bars” in these graphs represent one standard deviation of the data. Care must be exercised in using the standard deviation since only a limited number of repeats was performed and the nature of in-use emissions testing dictates that repeat runs were difficult to achieve. However, the spread of the data does allow for a discussion of the variability of the data. Fig. 8 compares the average reduction in the emissions due to the water injection system and Fig. 9 illustrates the average reduction in the emissions due to the switch of the fuels from conventional marine to LSD fuel, lower aromatic, higher cetane fuel.

From Fig. 4, the average power for each test condition appears to be repeatable. The data in this figure was influenced by the ocean and weather conditions, although there were no noticeable differences during the two days of testing. The greatest difference between the set point occurred for the 2000

rpm set point, an averaged difference of only 1.2%. From the data, it was difficult to determine if there was a cubic relationship between the shaft speed and engine power for the vessel's water jet propulsion system as would be found in conventional propeller propulsion systems; the vessel operators indicated that for the jet system the relationship was more linear than that for a direct propeller system.

The brake-specific fuel consumption, Fig. 5, was consistent at approximately 0.4 lb/bhp-hr for either fuel and with or without water injection. For the harbor tests with the marine fuel, the brake fuel consumption was dramatically higher due to low engine speed (650 rpm) and low power output. There does not appear to be a fuel penalty associated with using the low sulfur fuel or the water injection system.

The brake-specific mass emissions of NO_x and PM in Figs. 6 and 7, respectively, and in the comparisons in Figs. 8 and 9 shows that the PM was reduced by approximately 40% from the marine fuel to the LSD fuel while the vessel was underway. It is noted that there was a relatively large variation in the PM data for the 2100 rpm set point. There was no explanation for this variation. There may be a slight PM reduction when using the water injection system but it was not seen as being significant and was within the uncertainty of the experimental procedure. A significant reduction in NO_x was seen when the water injection system was used. The water injection system was activated only when the boost pressure was above a certain limit. Therefore, only the higher load set points had the water injection system activated. As seen in these two figures, the LSD fuel with water injection had a slightly higher reduction percentage than that of the marine fuel for a given set point. Also, there was a larger reduction percentage at lower engine speeds. This was due to the fact that there was a higher percentage of water injected at the lower engine speeds due to a constant water mass being injected when the system was activated. That is, there was no feedback or control on the amount of water injected into the intake; it was either on or off. The percentages shown in Fig. 9 for idle should be used with caution. There was a relatively large uncertainty in the data at idle due to the measurement equipment and the procedures used. Further testing would be warranted to draw any conclusive arguments on the idle data. Unfortunately, the large spread in the idle data was not found until after the testing was completed and it was not possible to retest the engine at idle due to budget constraints.

CONCLUSIONS

This effort evaluated the in-field mass rate and brake-specific mass emissions of NO_x and PM and fuel consumption for a high-speed ferry operating between Oceanside and San Diego, CA. For the water injection system, the brake-specific mass emissions of NO_x were reduced up to 16.5% and PM emissions were reduced by 40% using low sulfur diesel fuel and water injection compared to marine fuel. However, there was some uncertainty in the low sulfur fuel composition in that the LSD fuel was contaminated at some point during the testing or analysis and was not at the desired low sulfur level for the test. However, it should be recognized that even with this uncertainty, the LSD fuel that was reported had at least an order of magnitude lower sulfur level than the baseline marine fuel.

ACKNOWLEDGEMENTS

The authors acknowledge the dedicated support of organizations and individuals. Firstly, Stephen Goguen of the US Department of Energy, Office of FreedomCAR & Vehicle Technologies, is thanked for his support of the program. Bob Behr and Danny Gore from the Maritime Administration are thanked for providing technical support related to marine issues. Michael Winn and Lou Adamo from SCX, Inc are thanked for their logistical support. Ken Kimura at BP is thanked for providing the low sulfur diesel fuel. Anatoly Mezheritsky at M.A. Turbo/Engines is thanked for the installation of the water injection system. The Marine Services Express crew is acknowledged for their effort on pulling off the testing: Phillip Winter, captain Jim Saffer, mate Matt Hallisey, engineer Matt Rowley, and deckhand John Vierling. Finally, the faculty, staff, and students at West Virginia University are thanked for providing support to enable this work.

REFERENCES

1. M.A. Turbo/Engine, Ltd., Vancouver, BC.
2. "Control of Emissions From New and In-Use Highway Vehicles and Engines," Title 40 Code of Federal Regulations, Part 86, U.S. Government Printing Office, Washington, DC, 2000.
3. "Control of Emissions from New and In-Use Highway Vehicles and Engines," Title 40 Code of Federal Regulations, Part 89, U.S. Government Printing Office, Washington, DC, 2000.
4. "Control of Air Pollution From Locomotives and Locomotive Engines," Title 40 Code of Federal Regulations, Part 92, U.S. Government Printing Office, Washington, DC, 2000.
5. "Control of Emissions From Marine Compression-Ignition Engines," Title 40 Code of Federal Regulations, Part 94, U.S. Government Printing Office, Washington, DC, 2000.
6. Control of Emissions From New and In-Use Highway Vehicles and Engines Reciprocating Internal Combustion Engines – Exhaust Emissions Measurement," International Organization for Standardization, ISO/DIS 8178, Geneva, Switzerland, 1993.
7. "Measurement of Carbon Dioxide, Carbon Monoxide, and Oxides of Nitrogen in Diesel Exhaust," SAE Standard, SAE J177, Warrendale, PA 1995.
8. Behr, R., Gore, D., DeHart, J., Dr. Thompson, G., Gautam, M., Clark, N., Remley, W., and Corbett, J., "Advocating the Development of Universal Onboard Marine Emission Measurement Protocols," Proceedings of the Marine Environment Engineering Technology Symposium, Arlington, VA, 2003. See: <http://www.navalengineers.org>.
9. Corbett, J. J. and Robinson, A. L., "Measurements of NO_x Emissions and In-Service Duty Cycle from a Towboat Operating on the Inland River System," *Environmental Science and Technology*, 35, 2001.
10. Gautam, M., Clark, N. N., Thompson, G. J., and Lyons, D. W., "Assessment of Mobile Monitoring Technologies for Heavy-Duty Vehicle Emissions," Whitepaper Submitted to the Settling Heavy-Duty Diesel Engine Manufacturers,

Department of Mechanical and Aerospace Engineering, West Virginia University, Morgantown, WV, 1999. See: <http://www.epa.gov/Compliance/civil/programs/caa/diesel/test.html>.

Procedures for Heavy-Duty Diesel-Powered Vehicle Emissions," Phase II Final Report Submitted to the Settling Heavy-Duty Diesel Engine Manufacturers, Department of Mechanical and Aerospace Engineering, West Virginia University, Morgantown, WV, 2000. See: <http://www.epa.gov/Compliance/civil/programs/caa/diesel/test.html>.

11. Gautam, M., Clark, N. N., Thompson, G. J., Carder, D. K., and Lyons, D. W., "Evaluation of Mobile Monitoring Technologies for Heavy-Duty Diesel-Powered Vehicle Emissions," Phase I Final Report Submitted to the Settling Heavy-Duty Diesel Engine Manufacturers, Department of Mechanical and Aerospace Engineering, West Virginia University, Morgantown, WV, 2000. See: <http://www.epa.gov/Compliance/civil/programs/caa/diesel/test.html>.
12. Gautam, M., Clark, N. N., Thompson, G. J., Carder, D. K., and Lyons, D. W., "Development of In-use Testing

13. Gautam, G., Thompson, G. J., Carder, D. K., Clark, N. N., Shade, B. C., Riddle, W. C., and Lyons, D. W., "Measurement of In-Use, On-Board Emissions from Heavy-Duty Diesel Vehicles: Mobile Emissions Measurement System," SAE Technical Paper No. 2001-01-3643, 2001.

Table 3 Manual data collected from starboard forward and aft engines. Note that the 1900 rpm with LSD and WIS data were not collected. The horizontal line represents the two different test days. The data are also shown in the sequence in which it were collected.

Description	Seq No	Run No	GPS Spd	Forward Starboard Engine							Aft Starboard Engine				
				Eng Spd	Oil Pres	Water Temp	Exh Temp		Turbo Pres		Eng Spd	Oil Pres	Water Temp	Turbo Pres	
							T1	T2	P1	P2				P3	P4
			knts	RPM	psig	F	F	F	psig	psig	RPM	psig	F	psig	psig
2100 RPM, LSD	M010113	2		2100	60	180	635		18.7	19.2	2100	60	180	19.2	19.9
2100 rpm, LSD	M010113	3	37.0	2100	60	180	631		18.8	19.3	2100	60	180	19.0	19.4
2100 rpm, LSD, WIS	M010114	1	36.0	2100	60	180	617		18.9	19.3	2100	60	180	19.3	19.6
2100 rpm, LSD, WIS	M010114	2	33.6	2100	60	180	618		18.9	19.4	2100	60	180	19.1	19.6
2000 rpm, LSD, WIS	M010115	2	30.3	2000	60	180	600		15.8	16.2	2000	60	180	15.4	16.0
2000 rpm, LSD, WIS	M010115	3	32.6	2000	60	180	600		15.6	16.1	2000	60	180	15.2	15.8
2000 rpm, LSD	M010116	1	30.3	2000	60	180	-		15.3	15.6	2000	60	180	15.2	15.9
2000 rpm, LSD	M010116	2	28.8	2000	60	180	627		15.5	15.7	2000	60	180	15.1	15.6
1900 rpm, LSD	M010117	1	24.4	1900	60	170	600		12.3	12.6	2000	60	170	12.0	12.5
Idle, 650 rpm, LSD	M010118	1	0.0	670	25	120	137		0.1	0.1	670	25	120	0.2	0.2
Idle, 650 rpm, LSD	M010118	2	0.0	670	25	115	137		0.1	0.1	670	25	115	0.2	0.2
2100 rpm, Marine	M010119	1	35.6	2100	60	180	636		19.5	19.9	2100	60	180	19.8	20.2
2100 rpm, Marine	M010119	2	34.0	2100	60	180	632		18.7	19.2	2100	60	180	19.0	19.7
2100 rpm, Marine, WIS	M010120	1	33.0	2100	60	180	625		19.2	19.7	2100	60	180	19.7	20.3
2100 rpm, Marine, WIS	M010120	2	33.8	2100	60	180	621		19.4	19.8	2100	60	180	19.7	20.2
2000 rpm, Marine, WIS	M010121	1	28.6	2000	60	180	600		15.7	16.1	2000	60	180	15.1	15.9
2000 rpm, Marine, WIS	M010121	2	30.0	2000	60	180	597		15.7	16.2	2000	60	180	15.2	15.8
2000 rpm, Marine	M010122	1	29.2	2000	60	180	615		15.6	15.9	2000	60	180	15.3	15.9
2000 rpm, Marine	M010122	2	30.0	2000	60	180	617		15.5	15.9	2000	60	180	15.2	15.9
1900 rpm, Marine	M010123	1	25.5	1900	60	180	600		12.5	12.8	1900	60	180	12.5	12.5
1900 rpm, Marine	M010123	2	24.7	1900	60	180	602		12.5	12.8	1900	60	180	12.4	12.4
1900 rpm, Marine, WIS	M010124	1	25.0	1900	60	180	585		12.8	13.1	1900	60	180	12.3	12.3
1900 rpm, Marine, WIS	M010124	2	27.8	1900	60	180	585		12.8	13.1	1900	60	180	12.3	12.3
2100 rpm, Marine, WIS	M010125	1	32.2	2100	60	180	625		19.1	19.5	2100	60	180	19.1	19.1
650, Marine, Harbor, Temperature dropped through test	M010126	1	5.5	650	25	170	275-235		0.2	0.2	650	25	175	0.1	0.1
650, Marine, Harbor	M010127	1	3.2	650	25	125	190		0.2	0.1	650	25	125	0.3	0.3
2100 rpm, Marine, WIS	M010128	1	37.0	2100	60	180	620		19.2	19.5	2100	60	180	19.5	20.0
2100 rpm, Marine, WIS	M010128	2	35.5	2100	60	180	630		19.2	19.9	2100	60	180	19.7	20.1
2100 rpm, Marine, WIS	M010128	3	36.0	2100	60	180	628		19.3	20.0	2100	60	180	19.7	20.0
2100 rpm, Marine	M010129	1	31.5	2100	60	180	636		18.9	19.5	2100	60	180	19.2	19.7
2100 rpm, Marine	M010129	2	31.3	2100	60	180	636		19.0	19.5	2100	60	180	19.0	19.6
2100 rpm, Marine	M010129	3	31.8	2100	60	180	637		19.1	19.5	2100	60	180	19.0	19.7
650, Marine, Harbor, Temperature dropped through test	M010130	1	4.3	650	15	170	282-240		0.2	0.2	650	15	170	0.3	0.3
Idle, 650, Marine	M010131	1	0.0	650	12	120	143		0.5	0.5	650	0	0	0.0	0.0
Idle, 650, Marine	M010131	2	0.0	650	12	120	140		-	-	650	0	0	0.0	0.0

Table 4 Averaged run data for each configuration while underway. Note that the 1900 rpm LSD with WIS data were not collected.

Comment	Engine Speed rpm	GPS Speed mph	GPS Speed mph	Power hp	BSNOx g/bhp-hr	BSFC lb/bhp-hr	BSPM g/bhp-hr
2100 rpm LSD	2100	39.9	21.3	854.4	6.717	0.403	0.099
2100 rpm LSD WIS	2100	38.8	40.0	852.2	5.940	0.404	0.096
Marine 2100 rpm	2100	36.8	37.8	857.0	7.145	0.407	0.170
2100 rpm Marine WIS	2100	39.3	39.8	857.1	6.420	0.409	0.171
2000 rpm LSD	2000	35.4	34.0	737.7	6.451	0.397	0.112
2000 rpm LSD WIS	2000	35.9	36.2	737.7	5.512	0.401	0.105
2000 rpm Marine	2000	34.2	34.1	730.9	6.499	0.402	0.192
2000 rpm Marine WIS	2000	33.3	33.7	730.4	5.679	0.402	0.179
1900 rpm LSD	1900	28.8	28.1	620.4	5.969	0.399	0.160
1900 rpm LSD WIS							
1900 rpm Marine	1900	28.7	28.9	620.0	5.939	0.405	0.260
1900 rpm Marine WIS	1900	30.0	30.4	620.8	4.960	0.405	0.246
650 rpm Harbor Marine	650	4.4	5.0	20.9	18.416	0.896	0.159

Table 5 Averaged run data for each configuration while idle at the dock.

	Engine Speed rpm	GPS Speed mph	GPS Speed mph	Power hp	BSNOx g/hr	BSFC lb/hr	BSPM g/hr
LSD Idle	670	0	0	0	211	12.19	1.304
650 rpm Marine Idle	650	0	0	0	175	10.80	4.445

Table 6 Test fuels analysis report. The BP ECD® (LSD) fuel was contaminated. Care must be exercised when referencing this data to note this potential contamination.

Test	Units	Method	Fuel	
			LSD	Marine
API Gravity @ 60 Deg F	deg API	ASTM D-1298	39.2	34.7
Carbon	wt%	ASTM D-5291M	86.36	86.49
Cetane Index, Calculated	-	ASTM D-976	51.8	47
Cetane Number	-	ASTM D-613	53.1	46.1
Hydrogen Content	wt%	ASTM D-5291M	13.56	13.42
Kinematic Viscosity @ 40 deg. F	cSt	ASTM D-445	3.33	2.7
Specific Gravity	@ 60 deg.F	ASTM D-1298	0.8289	0.8514
Total Sulfur	wt%	ASTM D-4294	0.032	0.394
Distillation				
IBP	deg.F	ASTM D-86	365.6	347.9
5% Rec	deg.F		389.4	390.4
10% Rec	deg.F		401.2	413.4
20% Rec	deg.F		424.8	444.5
30% Rec	deg.F		447.3	469
40% Rec	deg.F		467.8	492
50% Rec	deg.F		492.1	514.1
60% Rec	deg.F		517.1	536.6
70% Rec	deg.F		542.8	559.7
80% Rec	deg.F		574.3	54.3
90% Rec	deg.F		612.5	623.3
95% Rec	deg.F		644.9	664.4
FBP	deg.F		667.2	676.4
Recovery	%		98.2	97.6
Residue	%		1.5	1.2
Loss	%		0.3	1.3
Flash Point, PMCC	deg.F	ASTM D-93(A)	140	136
Hydrocarbon Type - FIA		ASTM D-1319		
Aromatics	lv%		21.8	27
Olefins	lv%		0.8	0.7
Saturates	lv%		77.4	72.3

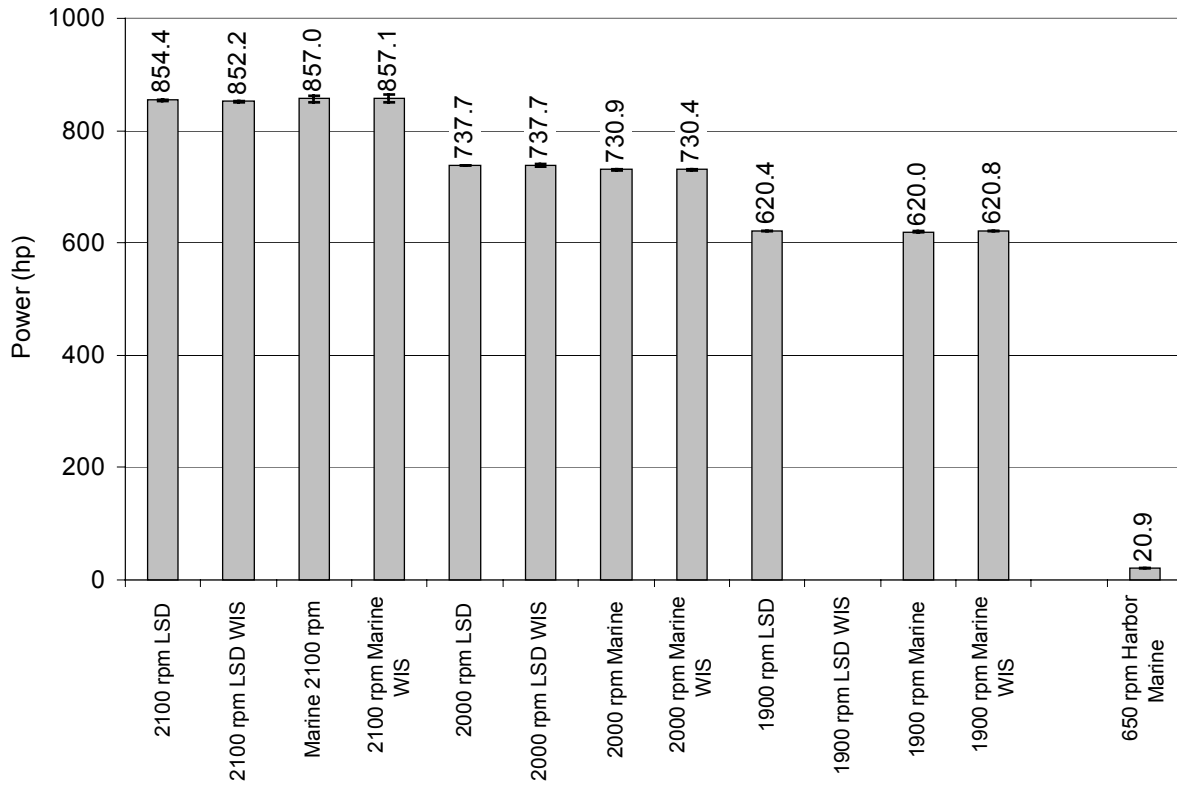


Fig. 4 Average power for each test configuration. Note that the 1900 rpm with LSD and WIS data were not collected.

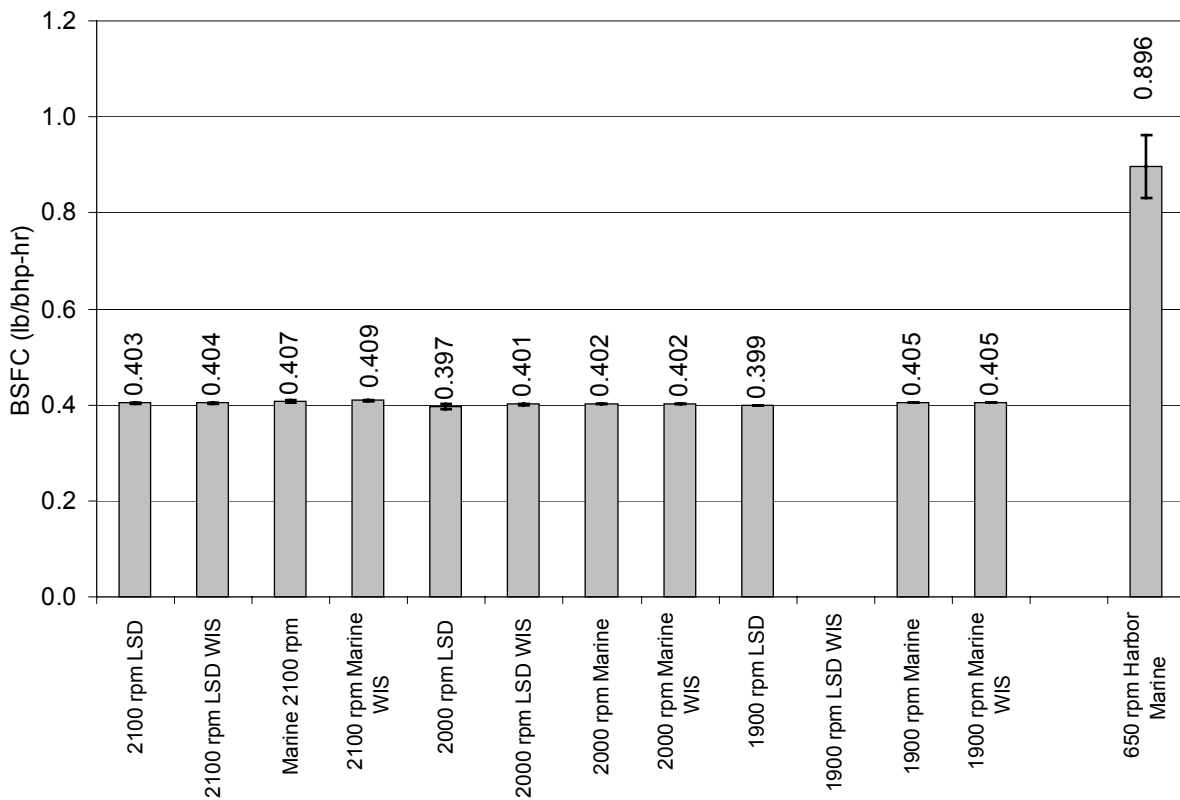


Fig. 5 Average brake-specific fuel consumption. Note that the 1900 rpm with LSD and WIS data were not collected.

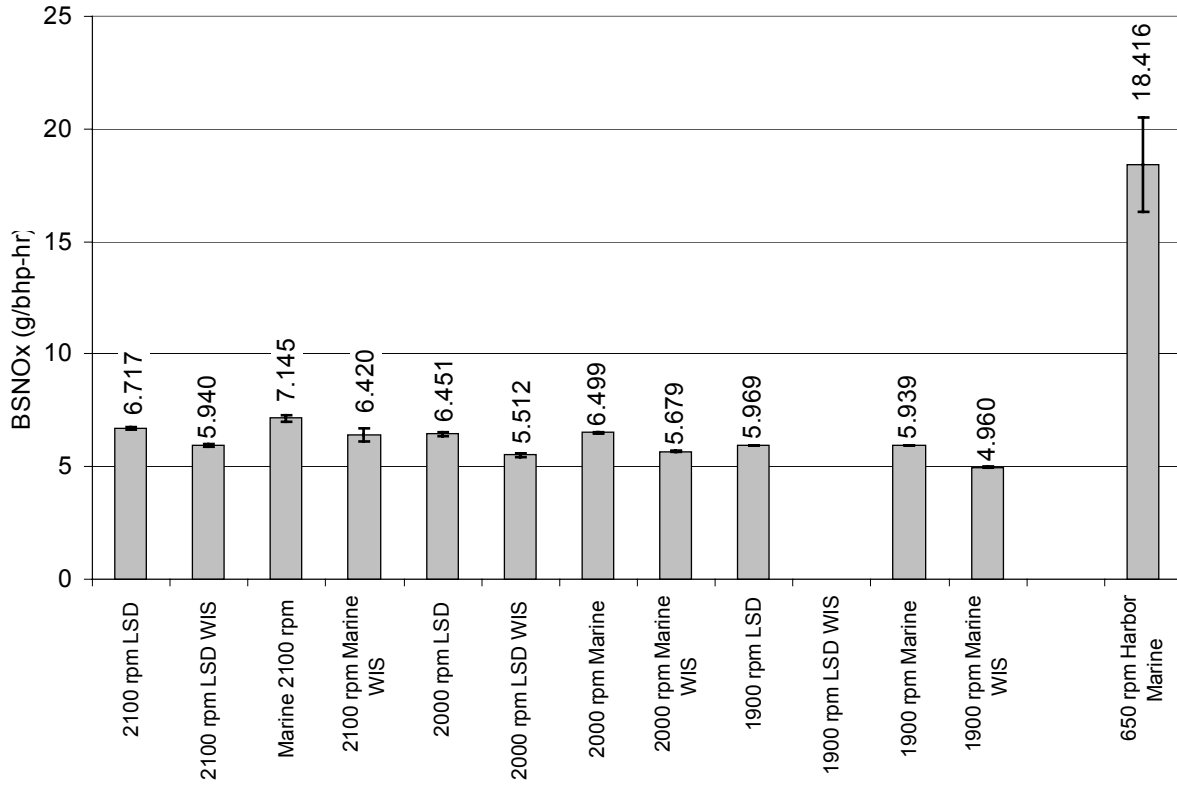


Fig. 6 Average brake-specific NOx emissions. Note that the 1900 rpm with LSD and WIS data were not collected.

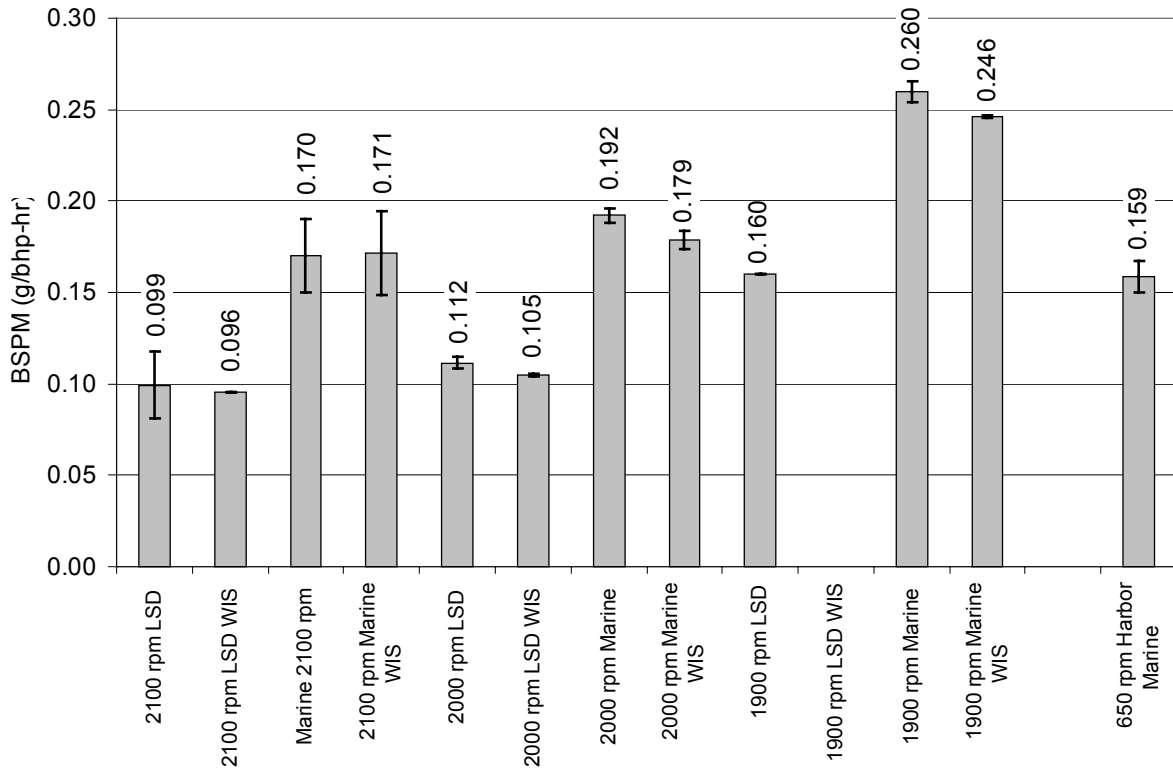


Fig. 7 Average brake-specific PM emissions. Note that the 1900 rpm with LSD and WIS data were not collected.

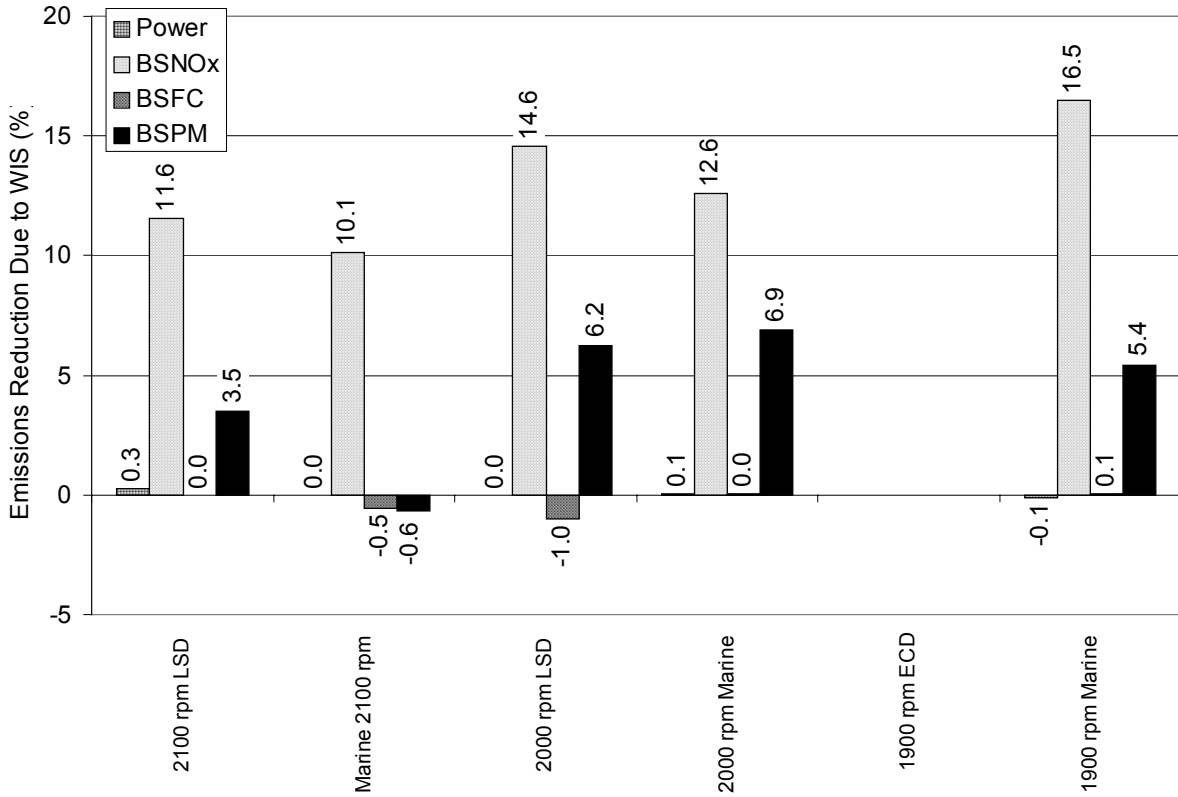


Fig. 8 Emissions reduction due to water injection. Note that the 1900 rpm with LSD and WIS data were not collected.

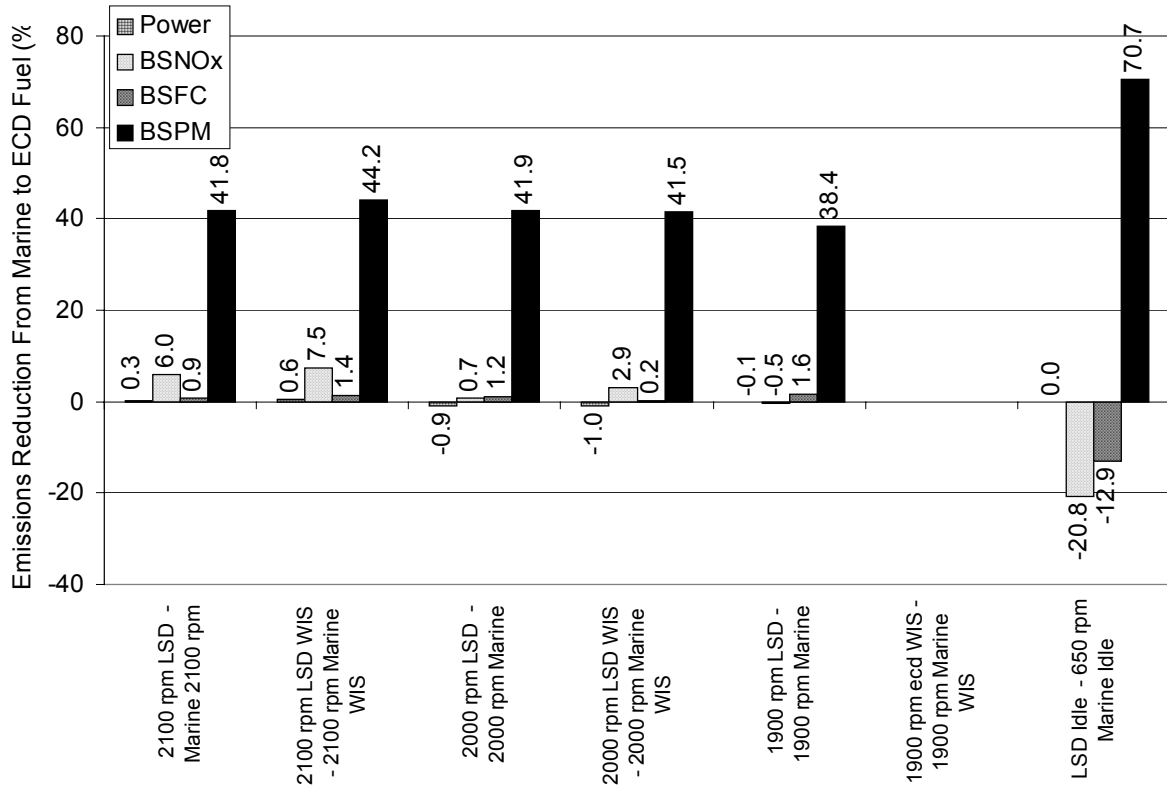


Fig. 9 Emissions reduction between marine and LSD fuel change. Note that the 1900 rpm with LSD and WIS data were not collected.